

MEASUREMENTS OF THE SCATTERING CHARACTERISTICS OF SEDIMENT SUSPENSIONS WITH DIFFERENT MINERALOGICAL COMPOSITIONS

Benjamin D. Moate ^{a*} and Peter D. Thorne ^a

^a Proudman Oceanographic Laboratory,
Joseph Proudman Building,
6, Brownlow Street,
Liverpool, L3 5DA, UK.

* Corresponding author: Dr. B.D. Moate, Email: bdm@pol.ac.uk, Tel: +44 (0) 151 795 4810

Abstract: *Acoustic studies of suspended sediments often assume the dominant mineral in suspension is quartz, the density and intrinsic scattering properties of which are implemented when inverting acoustic backscatter data collected at sea. However, compositional analysis studies of suspended and sea-bed particulate material show a wide range of mineral species contribute to the inorganic fraction of sediments in the marine environment. Whilst no theoretical framework exists to predict the acoustic properties of irregularly shaped sediment grains, the density, compressional, and shear wave velocities of common marine mineral species can vary by up to a factor of two. In this study, we present and compare measurements of the intrinsic scattering parameters, namely the normalized total scattering cross section, χ , and the backscatter form function, f , obtained from homogenous suspensions of irregularly shaped sand sized grains of both magnetite and quartz. Our preliminary measurements suggest that in the geometric scattering regime, χ is enhanced for magnetite sands by ~ 100 % relative to quartz. Similarly, measurements of the form function for magnetite sands are enhanced by ~ 33 % relative to quartz in the geometric regime, though no measurable difference was observed in the Rayleigh regime. The implications of these results for acoustic backscatter data collected at sea are discussed.*

Keywords: *Scattering, form function, cross section, sand, sediment, magnetite, mineralogy.*

MOATE, B.D., and THORNE, P.D., 2009. Measurements of the scattering characteristics of sediment suspensions with different mineralogical compositions. Conference Proceedings, 3rd International Conference and Exhibition on Underwater Acoustic Measurements: Technologies and Results, pg497-502, Nafplion, Greece, 21st-26th June 2009, ISBN 978-960-98883-4-9.

1. INTRODUCTION

Suspended marine sands significantly scatter underwater sound at MHz frequencies, with the suspended concentration and size controlling the backscattered intensity^{1,2,3}. Utilising this premise, monostatic Acoustic Backscatter Systems (ABS) have been developed over the past two decades, designed to collect profiles of suspended sediments in the bottom 1 – 2 m above the bed^{1,4}. Acoustics offer the advantages of non-intrusive measurements, with centimetric resolution, at turbulent and inter-wave timescales⁵.

In recent years, analytical inversions of multi-frequency ABS data have facilitated non-empirical estimates of suspended concentration and size^{4,6}. Such inversions require knowledge of the acoustic scattering properties of the particles, typically characterised by two dimensionless parameters; the backscatter form function, f , and normalised total scattering cross section, χ . Physically, f describes the backscattering characteristics of a particle relative to its geometrical size, whilst χ quantifies a particles total scattering over all angles, relative to its geometric cross section, and is proportional to particle scattering attenuation losses. For irregularly shaped particles such as natural sands, no analytical theoretical solution exists to describe χ and f . Consequently, to facilitate inversion of marine ABS data, χ and f have been determined experimentally for irregularly shaped quartz based sediments^{1,2,3}.

Compositional analysis studies of suspended and sea-bed particulate material however, show a wide range of mineral species contribute to the inorganic fraction of sediments in the marine environment^{7,8,9}. Mineralogically, sediments are usually divided into light and heavy fractions, based upon grain density, ρ . In marine sediments, commonly occurring light minerals include quartz, feldspar, calcite, mica and finer clay minerals, with common heavy minerals including garnet, ilmenite, magnetite, and zircon^{7,9,10,11,12}. Whilst many marine sediments consist of up to 95 % light minerals by mass, feldspar and calcite are often in equal or greater abundance than quartz in the silt to course sand size range^{8,9,13}. At the other extreme, heavy minerals such as magnetite and ilmenite can dominate the bulk sediment in some coastal and inter-tidal regions, giving rise to so-called black sands^{7,12,14}.

To date, no measurements of χ and f for non-quartz based sediments have been reported. Modelled scattering predictions for spheres having ρ , compressional, and shear wave velocities (V_P and V_S respectively) equal to those for garnet have been presented⁶, though it is unclear whether the differences imparted to χ and f due to mineralogy are significant, when compared to the enhanced scattering that occurs due to the irregular shape of marine particles relative to spheres. The aim of this study was to assess to what extent, if any, the intrinsic scattering properties of magnetite sands differ to those of quartz. Magnetite was chosen for study here as it is one of the heaviest minerals known to occur abundantly at some locations in the marine environment, with $\rho = 5196 \text{ kgm}^{-3}$, compared to 2650 kgm^{-3} for quartz.

2. MODELLING χ AND f

For a single size sphere of radius a , the theoretical far field χ and f are respectively^{15,16}:

$$\chi(x) = \frac{2}{x^2} \sum_{n=0}^{\infty} (2n+1) |b_n|^2 \quad (1)$$

$$f(x) = \frac{2}{ix} \sum_{n=0}^{\infty} (2n+1)(-1)^n b_n \quad (2)$$

where b_n is taken from the literature¹⁷, and $x = ka$, where $k = 2\pi/\lambda$, with λ the wavelength of sound in water. Evaluation of Equations 1 and 2 requires knowledge of ρ , V_P and V_S for each mineral, which were taken from the literature^{18,19}.

3. OBTAINING χ AND f FROM ABS MEASUREMENTS

Scattering measurements were obtained in a sediment tower, capable of generating homogenous suspensions for ABS studies^{3,20}. An AQUATEC® AQUAScat ABS operating at 0.5, 1, 2 and 4 MHz, was used to collect backscatter data at 0.01 m intervals over a range of 1.28 m. A pulse repetition frequency of 4 Hz was used to allow each transmission to fully dissipate before the next, with a system generated average produced every 32 pings, providing 1 recorded profile every 8 seconds. ABS data was collected from sands sieved into narrow $\frac{1}{4} \Phi$ size fractions, where $\Phi = -\text{Log}_2(d)$, with d the particle diameter in mm. $\frac{1}{4} \Phi$ size fractions comprise a nominally single size of sediments, thus enabling the measurement of the intrinsic scattering properties. To ensure the necessary size, shape, and purity characteristics were obtained, all sediments were sourced from commercial suppliers.

If the phase of the backscattered signal is randomly distributed over 2π , the root mean square backscattered voltage, V_{RMS} , can be shown to be⁵:

$$V_{RMS} = \frac{K_t M^{1/2} f}{r \psi \sqrt{a \rho}} e^{-2r\alpha} \quad (3)$$

where M is the mass concentration of suspended sediment, ψ accounts for the departure from spherical spreading in the transducer near field²¹, α is the total attenuation over the range r , and K_t is a system constant. K_t is obtained by calibration²⁰ and incorporates the receive sensitivity, electronic gain, and directivity of the transducer. The total attenuation includes contributions from water absorption, α_w , and sediment scattering losses, α_s , which add linearly, $\alpha = \alpha_w + \alpha_s$. The sediment scattering attenuation is proportional to χ :

$$\alpha_s = \frac{3\chi M}{4a\rho} \quad (4)$$

where all terms are as previously defined.

For a homogenous suspension, rearranging and taking the natural log transformation of Equation 3 yields a linear function of $\text{Log}_e(V_{RMS} r \psi)$ with range r from the transducer³:

$$\text{Log}_e(V_{RMS} r \psi) = \text{Log}_e\left(K_t M^{1/2} f / \sqrt{a \rho}\right) - 2r\alpha \quad (5)$$

Therefore, α_s can be obtained from the slope of Equation 5 by subtracting α_w (which can be taken from the literature²²). Providing M , ρ , and a are known, a profile mean value of χ can thus be calculated from Equation 4. In this way, accurate estimates of χ can be obtained providing $\alpha_s \geq \alpha_w$. Where $\alpha_s < \alpha_w$, small errors in the slope of Equation 5 reduce the accuracy of the estimated χ . This limitation, combined with the maximum sand concentration that would not damage the sediment tower pumps being $\sim 2 \text{ gl}^{-1}$, resulted in measurements of χ being obtainable at 4 MHz only. To utilise ABS data obtained at lower operating frequencies, f was calculated from the measured V_{RMS} by re-arranging Equation 3, and using a heuristic expression fitted to the measured χ to enable the computation of α_s at all frequencies.

4. RESULTS

Measurements of χ obtained from suspensions of the $\frac{1}{4} \Phi$ size fractions of magnetite and quartz sands are presented in Fig. 1a, along with heuristic fits to illustrate the general trends in the measurements. Theoretical predictions of χ for a $\frac{1}{4} \Phi$ distribution of spheres with the same ρ , V_P , and V_S characteristics as both magnetite and quartz are also shown in Fig. 1a. These theoretical predictions were obtained by evaluating Equation 1 over a uniform size distribution for $\frac{1}{4} \Phi$ size ranges of $a \pm 10\%$. Fig. 1a shows the measured χ for the magnetite sands were greater by up to $\sim 100\%$ in the geometric scattering regime ($x \gg 1$), relative to quartz sands. The measured χ for magnetite sands also showed significantly greater elevation when compared to the sphere predictions, then was observed for quartz.

Measurements of f obtained from the same suspensions are presented in Fig. 1b, again with heuristic fits to the measurements, and theoretical predictions obtained as above, using Equation 2. Fig. 1b shows the measured f obtained from magnetite sands were elevated relative to those obtained from quartz sands, by up to $\sim 33\%$ at $x \sim 2$, in the geometrical scattering regime. Measured f for magnetite sands also showed significantly greater elevation when compared to the sphere predictions, then was observed for quartz, at $x \geq 0.8$. However, below $x \sim 0.6$, in the Rayleigh scattering regime, there was no measurable difference in f between the magnetite and quartz, with measured f for both materials also being in closer agreement to the sphere predictions then at larger values of x .

5. DISCUSSION

These early results suggest that significant differences exist in the intrinsic scattering properties of irregularly shaped sands having different mineralogical compositions. Given the sphere predictions are similar in the region $x = 2 - 5$ (Fig. 1) for both materials studied, it is unclear why this similarity was not observed in the measured values of χ and f , with both being significantly elevated for the magnetite sands relative to quartz in this region. Some of the differences in observed scattering properties could conceivably be attributed to relative differences in the degree of departure of the magnetite and quartz grains from a spherical shape. Previous analysis of the quartz sands however have shown them to be highly irregularly shaped³, so this is considered to be an unlikely source of disagreement.

The observed differences in intrinsic scattering properties (Fig. 1) suggest that differences in mineralogical composition can significantly impact ABS data collected at sea. Given that at low values of x , χ and f for magnetite are similar to those for quartz, Equation 3 suggests that for suspensions of equal mass concentration and size, V_{RMS} for magnetite would be reduced by $\sim 1/\sqrt{2}$ relative to quartz, due to the higher density of magnetite (see Section 1). In contrast, at larger x , Equation 3 suggests V_{RMS} would be only slightly reduced, by $\sim 1.33/\sqrt{2}$. Further work is required to establish if differences in scattering properties exist between these materials and other commonly occurring marine mineral species, as well as to determine if these differences are significant in the presence of broad size distributions of sediment suspensions with mixed mineralogical compositions.

6. ACKNOWLEDGEMENTS

This work was jointly funded by the UK Natural Environment Research Council, as part of its small scale sediment process studies, and by the European HydralabIII-SANDS programme. The authors would like to thank AQUATEC SUBSEA Ltd for the loan of the 0.5 MHz transducer, and NORTHERN GEOLOGICAL SUPPLIES Ltd for the supply of the magnetite sands.

REFERENCES

- [1] Hay, A.E. Sound scattering from a particle-laden, turbulent jet. *J. Acoust. Soc. Am.*, 90 (4), 2055-2074, 1991.
- [2] He, C. and Hay, A.E. Broadband measurements of the acoustic backscatter cross section of sand particles in suspension. *J. Acoust. Soc. Am.*, 94 (4), 2247-1502, 1993.
- [3] Thorne, P.D. and Buckingham, M.J. Measurements of scattering by suspensions of irregularly shaped sand particles and comparison with a single parameter modified sphere model. *J. Acoust. Soc. Am.*, 116 (5), 2876-2889, 2004.
- [4] Thorne, P.D. and Hardcastle, P.J. Acoustic measurements of suspended sediments in turbulent currents and comparison with in-situ samples. *J. Acoust. Soc. Am.*, 101 (5), 2603-2614, 1997.
- [5] Thorne, P.D. and Hanes, D.M. A review of acoustic measurement of small-scale sediment processes. *Cont. Shelf Res.*, 22, 603-632, 2002.
- [6] Crawford, A.M. and Hay, A.E. Determining suspended sand size and concentration from multifrequency acoustic backscatter. *J. Acoust. Soc. Am.*, 94 (6), 3312-3324, 1993.
- [7] Boon, J.D. and Berquist, C.R. Jr. Evaluation of Sediment Dynamics and the Mobility of Heavy Minerals on a Linear Sand Shoal. *J. Coast. Res.*, 7 (4), 989-1002, 1991.
- [8] Jambers, W., Dekov, V. and Grieken, R.V. Single particle characterisation of inorganic and organic North Sea suspension. *Mar. Chem.*, 67, 17-32, 1999.
- [9] Friend, P.L., Velegrakis, A.F., Weatherston, P.D., and Collins, M.B. Sediment transport pathways in a dredged ria system, southwest England. *Est. Coast. Shelf Sci.*, 67, 491-502, 2006.
- [10] Al-Bakri, D., Khalaf, F., and Al-Ghadban, A. Mineralogy, genesis, and sources of surficial sediments in the Kuwait marine environment, Northern Arabian Gulf. *J. Sediment. Petrol.*, 54 (4), 1266-1279, 1984.
- [11] Poppe, L.J., Commeau, J.A., and Valentine, P.C. Mineralogy of the silt fraction in surficial sediments from the outer continental shelf off Southeastern New England. *J. Sediment. Petrol.*, 61 (1), 54-64, 1991.
- [12] Bryan, K.R., Robinson, A. and Briggs, R.M. Spatial and temporal variability of titanomagnetite placer deposits on a predominantly black sand beach. *Mar. Geol.*, 236, 45-59, 2007.
- [13] Soulsby, R. Dynamics of marine sands. *Thomas Telford*, 249pp, 1997.
- [14] Frihy, O.E. and Komar, P.D. Patterns of beach-sand sorting and shoreline erosion on the Nile Delta. *J. Sediment. Petrol.*, 61 (4), 544-550, 1991.
- [15] Hay, A.E. and Schaafsma, A.S. Resonance scattering in suspensions, *J. Acoust. Soc. Am.*, 85 (3), 1124-1138, 1989.
- [16] Thorne, P.D. and Campbell, S.C. Backscattering by a suspension of spheres. *J. Acoust. Soc. Am.*, 92 (2), 978-986, 1992.
- [17] Gaunard, G.C. and Uberall, H. RST analysis of monostatic and bistatic acoustic echoes from an elastic sphere. *J. Acoust. Soc. Am.*, 73 (1), 1-12, 1983.
- [18] Carmichael, R.S. Practical Handbook of Physical Properties of Rocks and Minerals, *CRC Press*, 741pp, 1990.
- [19] Reichmann, H.J. and Jacobsen, S.D. Sound velocities and elastic constants of $ZnAl_2O_4$ spinel and implications for spinel-elasticity systematics. *Am. Mineral.*, 91, 1049-1054, 2006.
- [20] Betteridge, K.F.E., Thorne, P.D. and Cooke, R.D. Calibrating multi-frequency acoustic backscatter systems for studying near-bed suspended sediment transport processes. *Cont. Shelf Res.*, 28, 227-235, 2008.
- [21] Downing, A., Thorne, P.D. and Vincent, C.E. Backscattering from a suspension in the near field of a piston transducer. *J. Acoust. Soc. Am.*, 97 (3), 1614-1620, 1995.
- [22] Kaye, G.W.C. and Laby, T.H. Tables of Physical and Chemical Constants, *Longman*, 477 pp, 1986.

Figures

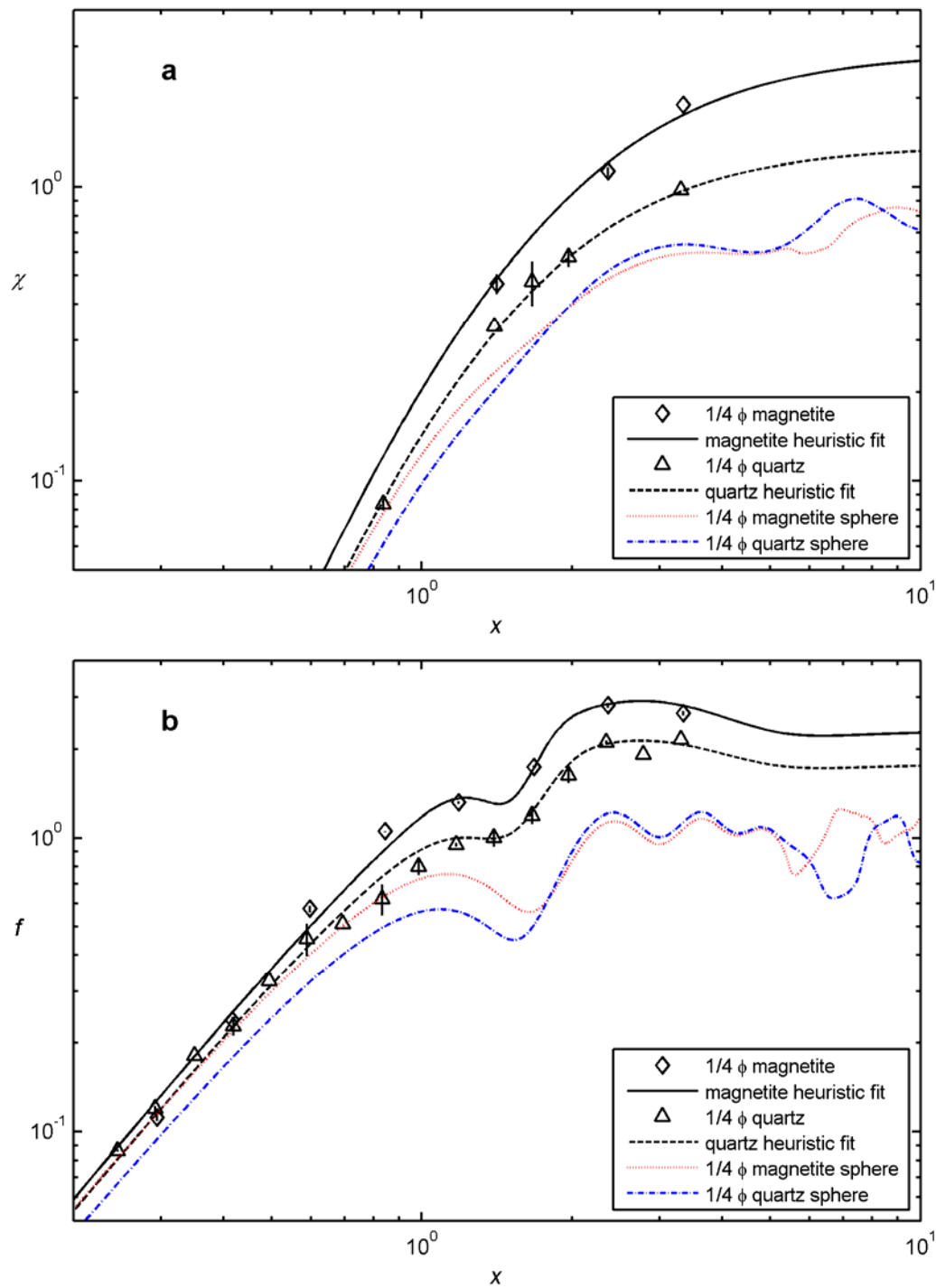


Fig. 1: Measurements of (a) χ and (b) f , obtained from $1/4 \Phi$ size fractions of magnetite and quartz sands. Heuristic fits to the measurements are also shown, along with theoretical predictions for $1/4 \Phi$ distributions of magnetite and quartz spheres.